

Morphology-controlled synthesis of silver nanoparticles on the silicon substrate by a facile silver mirror reaction

Bing Jiang,¹ Meicheng Li,^{1,3,a} Fan Bai,² Hang Yu,¹ Trevor Mwenya,¹ Yingfeng Li,¹ and Dandan Song¹

¹State Key Laboratory of Alternate Electrical Power System with Renewable Energy Sources, School of Renewable Energy, North China Electric Power University, China

²School of Materials Science and Engineering, Harbin Institute of Technology, China

³Suzhou Institute, North China Electric Power University, Suzhou 215123, China

(Received 10 December 2012; accepted 26 February 2013; published online 7 March 2013)

The Ag nanoparticles (Ag-NPs) with different morphology were quickly deposited on p-type Si substrate by a facile silver mirror reaction without capping agents and morphology driving seeds at room temperature. By controlling the concentrations of $[\text{Ag}(\text{NH}_3)_2]^+$ and reducing agent (glucose), short rod and quasi-round Ag-NPs were produced on Si substrate. The results show that the shape of the Ag-NPs was defined by $[\text{Ag}(\text{NH}_3)_2]^+$ concentration. The concentration of glucose affected the coverage fraction instead of shape of Ag-NPs. Under the high concentrations of $[\text{Ag}(\text{NH}_3)_2]^+$, anisotropic crystal structure of short rod Ag-NPs were ascribed to total energy minimization. The high glucose concentration led to agglomeration of particles. Different nanoporous structures on Si substrate etched by using Ag-NPs enable control over its properties and are useful for the solar cells applications. Copyright 2013 Author(s). This article is distributed under a Creative Commons Attribution 3.0 Unported License. [<http://dx.doi.org/10.1063/1.4794956>]

Metal-assisted chemical etching technique (MacEtch) has been used to prepare nanoscale structures on Si surface.¹⁻⁷ In solar cells application, the nanostructures on Si surface increase the antireflection effects, which in turn improve the efficiency of solar cells. In MacEtch, morphology of metal particles may affect the final etching nanostructures.^{4,5} Therefore, it is possible to control the nanostructure on the Si substrate by changing morphology of metal particles. In recent years, many studies have been dedicated to the nanostructure of metal particles for efficient utilization.⁸⁻¹² Silver is the most popular catalyst for MacEtch because of its good catalytic properties. In past decades, Ag-NPs in a variety of shapes have been successfully synthesized and nucleation and growth mechanisms have been proposed.¹³⁻²³ In most synthetic method, silver ions are reduced into Ag-NPs with many shapes by chemical process through introducing capping agents or shape-selected seeds. For MacEtch, Ag-NPs act as catalyst and they must be centrifuged, re-dispersed and re-coated on substrate. The process seems complex and not a one-step deposition on substrate. Additionally, capping agents might deactivate catalytic sites. Therefore, it is imperative to find a facile, direct and reproducible synthetic method to control morphology of Ag-NPs on the Si substrate for etching different nanostructures.

The silver mirror reaction is an “old” chemical route, which was used to generate reflective mirrors on solid supports.²⁴ In recent times, studies of nanotechnology have renewed the interest for this reaction. The silver mirror reaction has been used to prepare Ag-NPs, silver surfaces and core-shell structure on substrates for extensive applications.²⁵⁻³⁰ In this work, Ag-NPs were prepared in a single synthetic step on the Si substrate by a facile silver mirror reaction at room temperature without any capping agents and morphology driving seeds. The results show that Ag-NPs with controlled

^aAuthor to whom correspondence should be addressed. FAX: 86-10-6177-2951. Electronic mail: mcli@ncepu.edu.cn

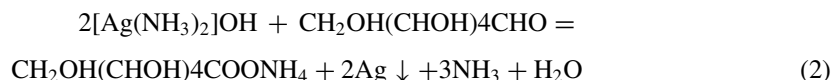


morphologies can be obtained by varying the concentrations of $[\text{Ag}(\text{NH}_3)_2]^+$ and reducing agent (glucose).

p-Si (100) single crystal wafers with resistivities of $\rho \sim 7\text{--}13 \Omega \text{ cm}$ were purchased from Emei Semiconductor Factory, China. Single-polished wafers were cut into $1.0 \times 1.0 \text{ cm}^2$ pieces and used for the experiments. Silver nitrate (AgNO_3), glucose ($\text{CH}_2\text{OH}(\text{CHOH})_4\text{CHO}$), aqueous ammonia ($\text{NH}_3 \cdot \text{H}_2\text{O}$, 28–30% NH_3), hydrofluoric acid (HF, 40%) and hydrogen peroxide (H_2O_2 , 30%) were purchased from Sinopharm Chemical Reagent Beijing Company. All these chemicals were reagent grade and deionized water was used to prepare all the aqueous solutions. AgNO_3 was dissolved in water and ethanol to form solutions. The $[\text{Ag}(\text{NH}_3)_2]\text{OH}$ solutions were prepared by reaction between AgNO_3 solution and aqueous ammonia. The aqueous ammonia was continuously dripped into the AgNO_3 solution while stirring until the solution became colorless. The reaction is as follow:



As well known, the silver mirror reaction actually is a redox reaction. In the reaction, the oxidizing $[\text{Ag}(\text{NH}_3)_2]^+$ were reduced to Ag-Nps by glucose with $-\text{CHO}$ aldehyde groups, as shown in Equation (2).



The concentrations of $[\text{Ag}(\text{NH}_3)_2]\text{OH}$ aqueous solutions were controlled at 0.2, 0.02 and 0.002M. Square polished p-type Si (100) samples of $10 \times 10 \times 0.5 \text{ mm}^3$ were cleaned by sonicating in solutions of 40% HF and deionized water. After that, the cleaned dry Si sample was put into the $[\text{Ag}(\text{NH}_3)_2]\text{OH}$ aqueous solution. Then specific amount of glucose (0.02, 0.01 and 0.005 M) was added into the $[\text{Ag}(\text{NH}_3)_2]\text{OH}$ aqueous solution while carefully stirring to ensure complete mixing. The reaction was kept at ambient temperature for 5 minutes and thereafter the Si sample with Ag-NPs was taken out and washed with concentrated HNO_3 and deionized water. The morphologies of Ag-NPs on the Si substrate were characterized by scanning electron microscope (SEM, FEI Quanta 200F) and atomic force microscope (AFM, Agilent 5500). The Ag-NPs on substrate were scraped off and observed by transmission electron microscope (TEM, FEI Tecnai G² F20). The Si samples with Ag-NPs were immersed into a mixing solution composed of HF, H_2O_2 and H_2O (1:5:2, volume ratio) for 5 minutes at ambient temperature. After the etching process, the Si samples were rinsed with deionized water and then immersed into concentrated HNO_3 for 10minutes to remove residual silver. The Si nanostructures were observed by SEM.

The morphology of the synthesized Ag-NPs on the Si substrate was studied using SEM. Table I shows the shape, size and coverage fraction of Ag-NPs prepared using varying concentrations parameters of $[\text{Ag}(\text{NH}_3)_2]^+$ and glucose. The results show that the shape of Ag-NPs depends on the concentrations of $[\text{Ag}(\text{NH}_3)_2]^+$. When the concentration of glucose was 0.01 or 0.005M, the changes in shape of Ag-NPs from irregular to quasi-round and then to short rod were induced by increase of $[\text{Ag}(\text{NH}_3)_2]^+$ concentration. When the concentration of glucose was 0.02M, the agglomerations of Ag-NPs were observed. The concentration of glucose affects the coverage fraction instead of the shape of Ag-NPs. The coverage fraction of Ag-NPs increased with increment of concentrations of glucose. Moreover, the size of Ag-NPs was influenced by both concentrations of $[\text{Ag}(\text{NH}_3)_2]^+$ and glucose. With 0.02M concentration of $[\text{Ag}(\text{NH}_3)_2]^+$, the sizes of Ag-NPs were larger and ranged between 60 and 100 nm. While under 0.2 and 0.002M concentration of $[\text{Ag}(\text{NH}_3)_2]^+$, the sizes of Ag-NPs were smaller and were about 30–40 nm. Increase in the concentration of glucose led to the agglomerations of Ag-NPs resulting in the increment in sizes.

Figure 1 presents micrographs of samples prepared using three different concentrations of $[\text{Ag}(\text{NH}_3)_2]^+$ when the concentration of glucose was 0.01M. Through EDS (Energy Dispersive Spectroscopy) analysis, the bright particles and dark areas in Figure 1 were defined as Ag particles and Si substrate, respectively. When the concentration of $[\text{Ag}(\text{NH}_3)_2]^+$ was 0.2M, most Ag-NPs displayed short rod shape, as shown in Figure 1(a). Figure 1(b) shows that the products were dominated by quasi-round Ag-NPs when the concentration of $[\text{Ag}(\text{NH}_3)_2]^+$ decreased to 0.02M. The

TABLE I. Various Ag-NPs under different concentration parameters.

$[\text{Ag}(\text{NH}_3)_2]^+$ (mol/L)	Glucose (mol/L)	Shape of Ag-NPs	Mean size of Ag-NPs (nm)	Coverage fraction of Ag-NPs (%)
0.002	0.02	irregular	30	24
0.002	0.01	irregular	30	18
0.002	0.005	irregular	30	15
0.02	0.02	agglomerate	100	59
0.02	0.01	quasi-round	60	44
0.02	0.005	quasi-round	60	31
0.2	0.02	agglomerate	100	57
0.2	0.01	short rod	40	44
0.2	0.005	short rod	40	33

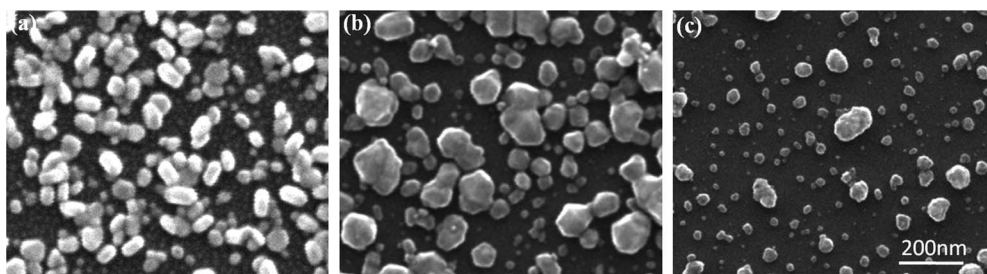
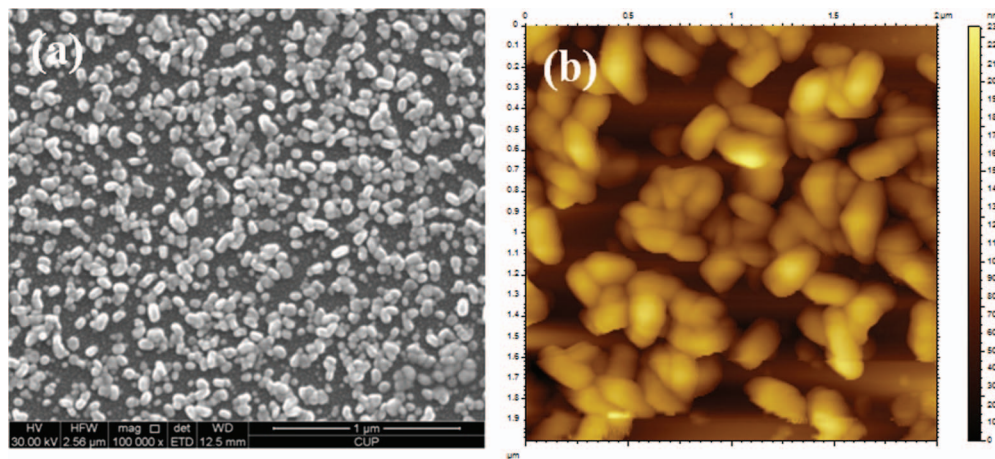
FIG. 1. SEM images of Ag-NPs on the Si substrate by varying the concentrations of $[\text{Ag}(\text{NH}_3)_2]^+$. (a) 0.2M: short rod; (b) 0.02M: quasi-round; (c) 0.002M: irregular.

FIG. 2. Morphology of short rod Ag-NPs observed by (a) SEM and (b) AFM.

Ag-NPs having irregular shape were observed when the $[\text{Ag}(\text{NH}_3)_2]^+$ concentration was 0.002M, as shown in Figure 1(c). The results show that the concentration of $[\text{Ag}(\text{NH}_3)_2]^+$ plays an important role in the shape of Ag-NPs. From Table I and Figure 1, the anisotropic growth of Ag-NPs was induced by increasing the concentration of $[\text{Ag}(\text{NH}_3)_2]^+$. That is, anisotropic short rod Ag-NPs can be attained easily in solutions with a high concentrations of $[\text{Ag}(\text{NH}_3)_2]^+$. Figure 2 shows the morphology of short rod Ag-NPs using SEM and AFM. Through observation, the Ag nanorods displayed anisotropic and had a uniform distribution with about 40 nm in size.

Figure 3 shows TEM images of the short rod and quasi-round particles scraped from the samples in Figure 1(a) and 1(b). Multiply twinned structure was observed in a small quasi-round particle. In the literature, a five-fold twinned, decahedral seed consist of five single-crystal, tetrahedral units

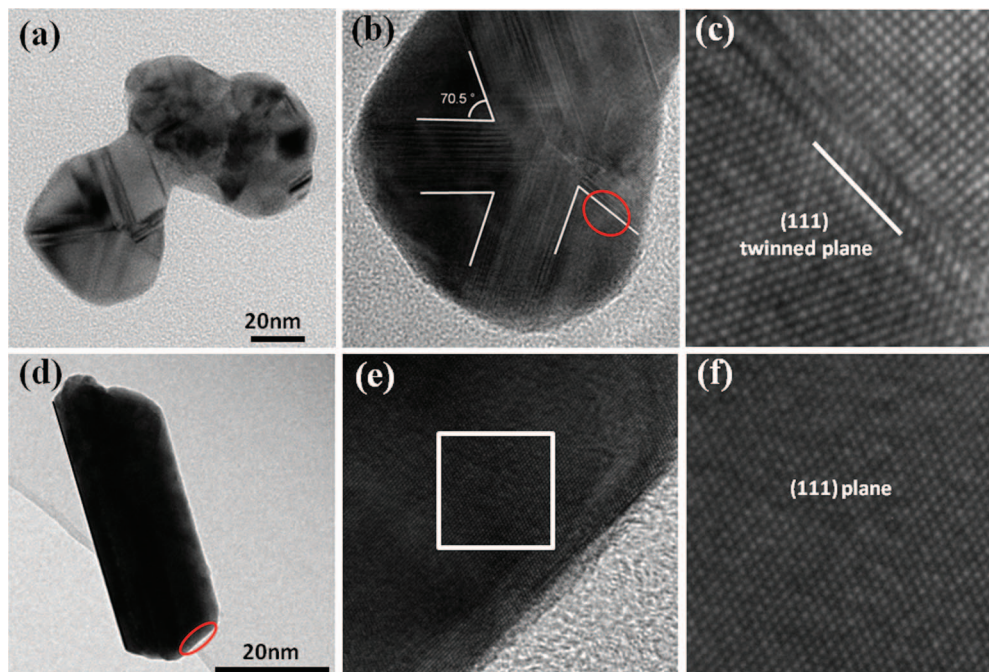


FIG. 3. HRTEM images of short rod and quasi-round Ag-NPs. (a) (b) (c) morphology and HRTEM images of quasi-round Ag-NPs; (d) (e) (f) morphology and HRTEM images of short rod Ag-NPs.

through $\{111\}$ twinned planes. The theoretical angle between two $\{111\}$ twinned planes is 70.53° .²⁰ Multiply twinned seeds are favored by thermodynamics because they have more $\{111\}$ planes with the lower surface energy. From Figure 3(a)–3(c), the exposed $\{111\}$ crystal facets are joined by twinned planes and the angle between two twinned planes is about $70.5^\circ \pm 0.3^\circ$. The high-resolution TEM images of crystal facets and twinned planes are shown in Figure 3(c). The result shows that quasi-round Ag-NPs were products derived from multiply twinned seeds under the low $[\text{Ag}(\text{NH}_3)_2]^+$ concentration (0.02M) without capping agents.

The high-resolution TEM images show that the top edge of a short rod particle is $\{111\}$ plane, as shown in Figure 3(d)–3(f). Xia *et al.* have given many growth pathways of Ag-NPs.²³ Combining the analysis of reaction pathways and TEM observation, the short rod Ag-NPs may be five-fold twinned rod, which is induced by anisotropic growth of multiply twinned seeds. In our experiments, the Ag-NPs were quasi-round when the mol ratio of $[\text{Ag}(\text{NH}_3)_2]^+$ and glucose was 2:1, which is according to reaction as Equation (2) (See Table I). When the concentrations of $[\text{Ag}(\text{NH}_3)_2]^+$ was 0.2M, the mol ratio was much higher than 2:1, that is, the amount of $[\text{Ag}(\text{NH}_3)_2]^+$ was excessive (See Table I). These results show that the excessive $[\text{Ag}(\text{NH}_3)_2]^+$ aggravated the anisotropic growth of multiply twinned seeds, resulting in the formation of short rod Ag-NPs. Generally, the reaction rate of high concentrations is higher than that of low concentrations, resulting in the smaller size of particles. In our experiments, the size of Ag nanorods was smaller than that of quasi-round Ag-NPs (see Figure 1 and Table I). Figure 4 depicts the growth process of a Ag nanorod under the high concentration of $[\text{Ag}(\text{NH}_3)_2]^+$ (0.2M). With increment of time, the Ag-NPs grew from a five-fold twinned decahedron to a five-fold twinned rod. Schematic images of the evolution of a five-fold twinned rod are depicted in Figure 4(d). The results show that the rate of reaction of the high concentrations of $[\text{Ag}(\text{NH}_3)_2]^+$ was higher than that of low concentrations.

With high $[\text{Ag}(\text{NH}_3)_2]^+$ concentration (0.2M), the seeds would expand rapidly in size. Theoretically, the seed should be favored to grow in $\{111\}$ planes that reduce the surface energy. However, strain energy of twinned planes will be greatly increased when the seed grows laterally. In this condition, the low surface energy of $\{111\}$ facets can no longer remedy the excessive strain energy during rapid growth. By contrast, elongation along the direction parallel to the twinned planes does not

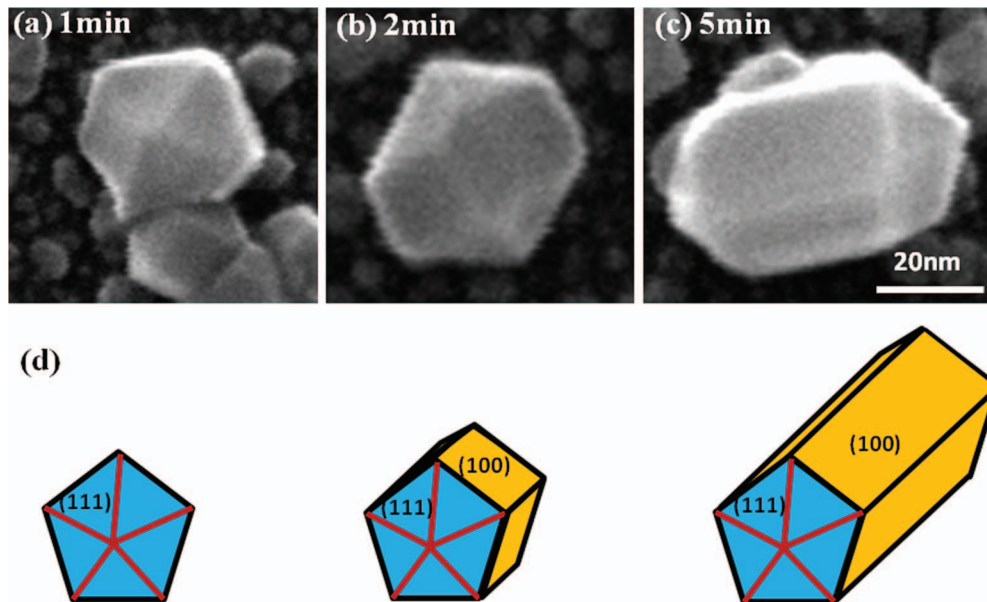


FIG. 4. The growth of Ag nanorod under the high concentrations of $[\text{Ag}(\text{NH}_3)_2]^+$ (0.2M) (a) a five-fold twinned decahedron; (b) a five-fold twinned icosahedron; (c) a five-fold twinned rod; (d) schematic images of the growth process of a five-fold twinned rod.

lead to increase of strain energy. Therefore, the seeds would preferentially grow along the direction parallel to the twin planes to lower the total interfacial free energy. The energy minimization is the driving force for the quick formation of nanorods under the high concentrations of $[\text{Ag}(\text{NH}_3)_2]^+$.

The Ag-NPs can be used to etch nanostructure on the Si substrate by MacEtch, i.e. nanoporous and nanowires.^{1-7,31-34} These different nanostructures can be used in antireflection layer of solar cell devices. In etching process, the nanostructure can be controlled by changing the morphology of Ag-NPs. In this work, the effect of morphology of Ag-NPs on etching structure of Si substrate was investigated. Figure 5 presents nanoporous etched by shot rod and quasi-round Ag-NPs. The results show that round porous were easily etched by quasi-round Ag-NPs while small irregular-shaped porous were obtained by shot rod Ag-NPs. Meanwhile, the more round porous were obtained by enhancing coverage fraction of quasi-round Ag-NPs. Through SEM observation, it was found that the morphology of Ag-NPs had effect on the etching structure under the same etching process. The properties and catalysis mechanism of different nanostructures by varying morphology will be intensively studied in the future.

In summary, shot rod and quasi-round Ag-NPs can be directly prepared on the Si substrate at room temperature by a facile silver mirror reaction without any capping agents and morphology driving seeds. The results show that the morphology of Ag-NPs could be controlled by varying the concentrations of $[\text{Ag}(\text{NH}_3)_2]^+$ and reducing agent (glucose). The shapes of Ag-NPs were influenced by the concentrations of $[\text{Ag}(\text{NH}_3)_2]^+$, whereas the coverage fraction of Ag-NPs was related to the glucose concentration. Multiply twinned seeds grew to quasi-round Ag-NPs under the relatively lower $[\text{Ag}(\text{NH}_3)_2]^+$ concentrations. The rapid growth under the higher $[\text{Ag}(\text{NH}_3)_2]^+$ concentrations aggravated the anisotropic growth of multiply twinned seeds, resulting in the formation of short rod Ag-NPs. The driving force of anisotropic growth is total energy minimization. Our research has provided a facile synthetic process of Ag-NPs with different morphology, which has many advantages including the simplicity of one-step chemical procedure, the absence of capping agents and morphology driving seeds, and direct quickly preparation on the substrate. Moreover, the experimental results show that morphology of Ag-NPs had an effect on the etching nanostructure on Si substrate. Different nanostructures can be used to adjust the antireflection properties of Si surface in solar cell devices.

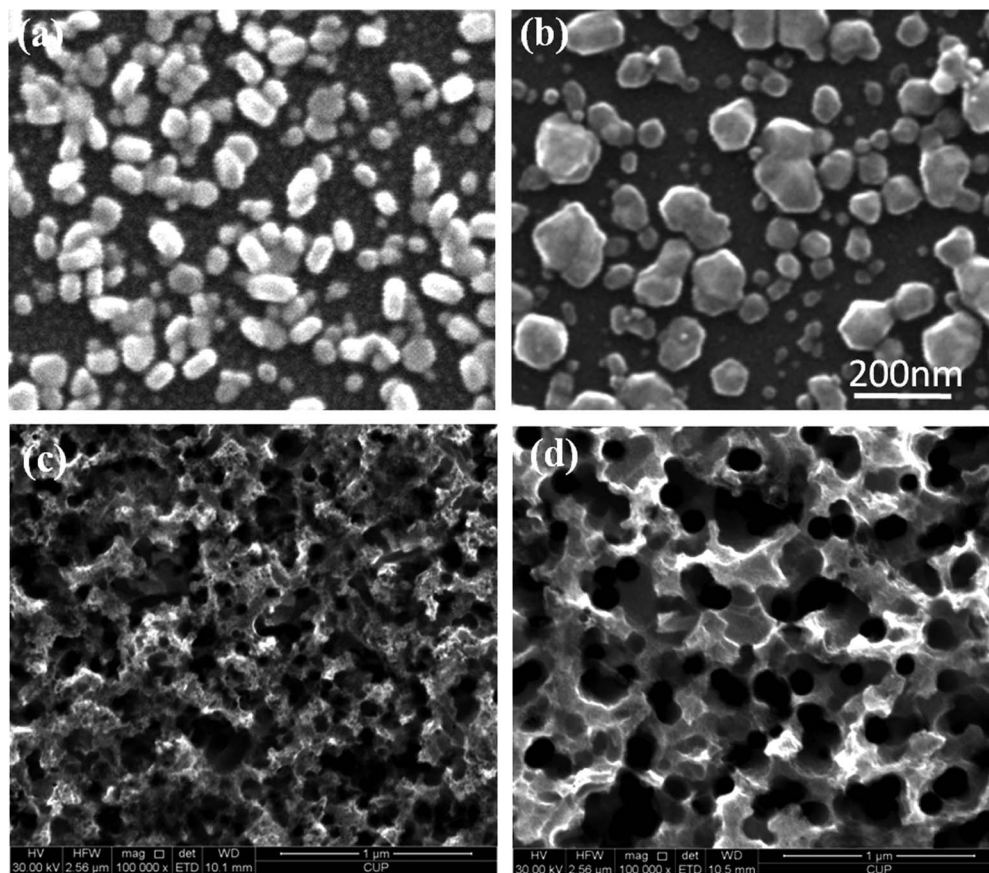


FIG. 5. The Si nanoporous etched by Ag-NPs with different shapes. (a) short rod Ag-NPs; (b) quasi-round Ag-NPs; (c) nanoporous etched by short rod Ag-NPs; (d) nanoporous etched by quasi-round Ag-NPs.

ACKNOWLEDGMENT

The authors acknowledge support of the National Natural Science Foundation of China (Grant No. 51202067, 51172069, 50972032 and 61204064), Ph.D Programs Foundation of Ministry of Education of China (20110036110006) and the Fundamental Research Funds for the Central Universities (11ZG02, 12QN15).

- ¹ X. Li and P. W. Bohn, *Appl. Phys. Lett.* **77**, 2572 (2000).
- ² H. Chen, R. Zou, H. Chen, N. Wang, Y. Sun, Q. Tian, J. Wu, Z. Chen, and J. Hu, *J. Mater. Chem.* **21**, 801 (2011).
- ³ H. Park, S. Choi, J.-P. Lee, and S. Park, *J. Mater. Chem.* **21**, 11996 (2011).
- ⁴ X. W. Geng, M. C. Li, L. C. Zhao, and P. W. Bohn, *J Electron Mater.* **40**, 2480 (2011).
- ⁵ Z. Huang, N. Geyer, P. Werner, J. De Boor, and U. Gösele, *Adv. Mater.* **23**, 285 (2011).
- ⁶ F. Bai, M. Li, D. Song, H. Yu, B. Jiang, and Y. Li, *J. Solid State Chem.* **196**, 596 (2012).
- ⁷ F. Bai, M. Li, R. Huang, D. Song, B. Jiang, and Y. Li, *Nano. Res. Lett.* **7**, 557 (2012).
- ⁸ M. Cheng and J. Yang, *Appl. Spectrosc.* **62**, 1384 (2008).
- ⁹ M. J. Banholzer, J. E. Millstone, L. Qin, and C. A. Mirkin, *Chem. Soc. Rev.* **37**, 885 (2008).
- ¹⁰ S. H. Han, L. S. Park, and J.-S. Lee, *J. Mater. Chem.* **22**, 20223 (2012).
- ¹¹ Bhaskar R. Sathe, *AIP Advances* **2**, 042122 (2012).
- ¹² H. Dai, M. Li, Y. Li, H. Yu, F. Bai, and X. Ren, *Optics Express* **20**, A503 (2012).
- ¹³ J. Bonsak, J. Mayandi, A. Thøgersen, E. Stensrud Marstein, and U. Mahalingam, *Phys. Status. Solidi (c)* **8**, 924 (2011).
- ¹⁴ J. Zeng, Y. Zheng, M. Rycenga, J. Tao, Z. Y. Li, Q. Zhang, Y. Zhu, and Y. Xia, *J. Am. Chem. Soc.* **132**, 8552 (2010).
- ¹⁵ P. Gangopadhyay, P. Magudapathy, S. K. Srivastava, K. G. M. Nair, and B. K. Panigrahi, *AIP Advances* **1**, 032112 (2011).
- ¹⁶ J. Zeng, X. Xia, M. Rycenga, P. Henneghan, Q. Li and Y. Xia, *Angew. Chem., Int. Ed.* **50**, 244 (2011).
- ¹⁷ B. J. Wiley, Y. Chen, J. M. McLellan, Y. Xiong, Z. Li, D. Ginger, and Y. Xia, *Nano Lett.* **7**, 1022 (2007).
- ¹⁸ D. Yu and V. W. Yam, *J. Phys. Chem. B.* **109**, 5497 (2005).

- ¹⁹H. Liang, H. Yang, W. Wang, J. Li, and H. Xu, *J. Am. Chem. Soc.* **131**, 6068 (2009).
- ²⁰B. Wiley, Y. Sun, B. Mayers, and Y. Xia, *Chem. Eur. J.* **11**, 454 (2005).
- ²¹A. M.E. Kamel and M. E.A. Hassan, *Int. J. Nanomed.* **7**, 1543 (2012).
- ²²M. M. Mariscal, J. J. Velazquez-Salazarb, and M. J. Yacaman, *Cryst. Eng. Comm.* **14**, 544 (2012).
- ²³Y. Xia, Y. Xiong, B. Lim, and S. E. Skrabalak, *Angew. Chem. Int. Ed.* **47**, 2 (2008).
- ²⁴A. G. Ingalls, *Amateur Telescope Making (Book One)* (Scientific American Inc., New York, 1981). p 101.
- ²⁵R. Dondi, W. Su, G. A. Griffith, G. Clark, and G. A. Burley, *Small* **8**, 770 (2012).
- ²⁶X. Li, J. Shen, A. Du, Z. Zhang, G. Gao, H. Yang, and J. Wu, *Colloids and Surfaces A: Physicochem. Eng. Aspects.* **400**, 73 (2012).
- ²⁷Y. Saito, J. J. Wang, D. N. Batchelder, and D. A. Smith, *Langmuir* **19**, 6857 (2003).
- ²⁸L. Shen, J. Ji, and J. Shen, *Langmuir* **24**, 9962 (2008).
- ²⁹T. V. Bukreeva, I. V. Marchenko, B. V. Parakhonskiy, and Y. V. Grigor'ev, *Colloid Journal* **71**, 596 (2009).
- ³⁰Z. Xu, J. Hao, F. Li, and X. Meng, *J. Colloid Interf. Sci.* **347**, 90 (2010).
- ³¹K. Tsujino and M. Matsumura, *Electrochim Acta* **53**, 28 (2007).
- ³²S. Yae, Y. Morii, N. Fukumuro, and H. Matsuda, *Nano. Res. Lett.* **7**, 352 (2012).
- ³³C.-L. Lee, K. Tsujino, Y. Kanda, S. Ikeda, and M. Matsumura, *J. Mater. Chem.* **18**, 1015 (2008).
- ³⁴Z. Huang, X. Zhang, M. Reiche, L. Liu, W. Lee, T. Shimizu, S. Senz, and U. Gosele, *Nano. Lett.* **8**, 3046 (2008).